







Open Archive TOULOUSE Archive Ouverte (OATAO)

OATAO is an open access repository that collects the work of Toulouse researchers and makes it freely available over the web where possible.

This is an author-deposited version published in : <http://oatao.univ-toulouse.fr/>
Eprints ID : 19639

To link to this article : DOI:10.1007/s00348-009-0732-4

URL : <http://dx.doi.org/10.1007/s00348-009-0732-4>

To cite this version : Lacaze, Laurent  and Brancher, Pierre  and Eiff, Olivier  and Labat, Ludovic  *Experimental characterization of the 3D dynamics of a laminar shallow vortex dipole.* (2010) Experiments in Fluids, vol. 48 (n° 2). pp. 225-231. ISSN 0723-4864

Any correspondence concerning this service should be sent to the repository administrator: staff-oatao@listes-diff.inp-toulouse.fr

Experimental characterization of the 3D dynamics of a laminar shallow vortex dipole

Laurent Lacaze · Pierre Brancher ·
Olivier Eiff · Ludovic Labat

Abstract Experimental results on the dynamics of a vortex dipole evolving in a shallow fluid layer are presented. In particular, the generation of a spanwise vortex at the front of the dipole is observed in agreement with previous experiments at larger Reynolds numbers. The results show that this secondary vortex is of comparable strength to the dipole. The present physical analysis suggests that the origin of this structure involves the stretching induced by the dipole of the boundary-layer vorticity generated by the dipole's advection over the no-slip bottom.

1 Introduction

Vortex dipoles are hydrodynamic structures composed of two aggregated counter-rotating vortices that are observed in geophysical flows such as tidal estuaries (Fujiwara et al. 1994; Wells and van Heijst 2003) or rip currents (Smith and Largier 1995; Peregrine 1998). The transport of pollutants or sediments by such structures is a critical environmental issue in these configurations as vortex dipoles are expected to transport mass (and momentum) over long distances. In the case of rip currents for instance, this mass transport can lead to the deformation of the sand bed and ultimately to a modification of the sea-floor bed topography.

Many laboratory experiments have shown that quasi-two-dimensional vortex dipoles are generically produced by the collapse of initially three-dimensional turbulent jet-like flows when submitted to specific constraints such as a density stratification (Voropayev et al. 1991; Flór et al. 1995) or a small fluid-layer thickness (Sous et al. 2004; Voropayev et al. 2007). In Voropayev et al. (2007) and Sous et al. (2004), an impulsive jet in a shallow layer of water is used to mimic the aforementioned geophysical flow configurations. The quasi two-dimensional decay of the initially turbulent flow is observed together with the generation of vertical motions at the front of the dipole. More specifically the experimental observations suggest the presence of a horizontal spanwise vortex, a feature contradicting the quasi-two-dimensional hypothesis classically put forward for the description of such shallow flows. Such a spanwise vortex is expected to dramatically affect the dissipation rate as well as the mixing and transport properties of the overall structure. Lin et al. (2003) have carried out experiments on the three-dimensional dynamics of vortex dipoles directly generated by a piston in a shallow layer of fluid. They uncovered intricate three-dimensional vortex structures whose complexity presumably originates from transition and separation mechanisms activated at the relatively large Reynolds numbers investigated in their study. More recently, Akkermans et al. (2008a, b) have performed similar experiments in which the vortex dipole was created using a magnetic source, as in Afanasyev and Korabel (2006). More precisely, these studies focused on the three-dimensional flow taking place within the core of the counter-rotating vortices forming the dipole.

In that context, we have started an experimental investigation of the three-dimensional dynamics of a laminar vortex dipole evolving in a shallow layer of water on a

L. Lacaze (✉) · P. Brancher · O. Eiff · L. Labat
Université de Toulouse; INPT, UPS; IMFT (Institut de
Mécanique des Fluides de Toulouse); Allée Camille Soula,
31400 Toulouse, France
e-mail: lacaze@imft.fr

L. Lacaze · P. Brancher · O. Eiff · L. Labat
CNRS; IMFT; 31400 Toulouse, France

rigid, flat, and smooth surface. The present study aims at clarifying the role of the boundary layer associated with the no-slip condition at the solid bottom—and the subsequent vertical shear—in the development of the three-dimensional motions observed in Lin et al. (2003) and Sous et al. (2004).

2 Experimental setup

Figure 1 shows a sketch of the experimental setup. Experiments have been performed in a rectangular tank ($L \times W = 2 \text{ m} \times 1 \text{ m}$) filled with water at rest. The depth of the water layer is $H = 2.5 \text{ cm}$ for all the experiments presented here. The dipole is generated directly by the rotation of two vertical flaps. The same technique has been used in several experiments of columnar vortex pairs (Lewke and Williamson 1998; Meunier and Lewke 2005): two vertical plates, initially parallel, are put into rotation along a vertical axis with a linearly decreasing rotation rate and a closing angle as described in Billant and Chomaz (2000) in order to minimize the influence of the small stopping vortices created at the end of the flaps' motion. Moreover the gap between the rotating flaps and the bottom has been carefully bridged by a foam rubber to avoid the generation of secondary flows that could have perturbed the dipole formation and altered its subsequent evolution.

For a fixed closing angle and initial flap distance, the generation procedure is parameterized by the closing-time T which was chosen long enough to prevent any unwanted source of asymmetry, turbulent or not, that would inevitably occur at high rotation speed. For closing-times T between 10 and 15 s presented here, the roll-up of the shear layer at the moving edge of the flaps produces laminar

vortex dipoles with typical size $D \sim 8 \text{ cm}$ and velocity $U \sim 3 \text{ mm/s}$ (Fig. 1).

The present flow has three characteristic length scales: the dipole diameter D , the water layer depth H and the boundary layer thickness δ . Therefore, several Reynolds numbers can be defined. With an exhaustive parametric study still lacking, it is not obvious to know a priori which definition is the most relevant. In that context, the different Reynolds numbers are given in the following for the sake of completeness. The ratio between the (vertical) viscous diffusion time H^2/ν and the (horizontal) advection time U/D defines a Reynolds number for our experiments as $Re = \eta Re_H = \eta^2 Re_D$, where $\eta = H/D$ is the height-to-width aspect ratio of the dipole, $Re_H = UH/\nu$ is the (vertical) Reynolds number based on the thickness of the fluid layer of viscosity ν , and $Re_D = UD/\nu$ is the (horizontal) Reynolds number associated with the horizontal diffusion of the quasi-two-dimensional dipolar structure. In the present experiments, typical values of η , Re_H , Re_D , and Re are, respectively, 0.3, 75, 240 and 20. Note that these Reynolds numbers are an order of magnitude lower than in the experimental study of Lin et al. (2003). We therefore expect the dynamics to be relatively simpler in the present case. More particularly, the self-induced propagation at velocity U of a vortex dipole of characteristic length D generates a boundary layer whose thickness δ can be roughly estimated via a balance between the vertical diffusion and the horizontal advection times of the momentum, i.e., $\delta^2/\nu = D/U$. The boundary layer thickness is then $\delta = H/\sqrt{Re}$ with a typical value of $\delta \sim 5 \text{ mm}$ for the experiments presented here. This corresponds to a boundary layer Reynolds number $Re_\delta = U\delta/\nu$ of about 15, which suggests that the boundary layer is stable and laminar. In all the experiments reported here, we observed symmetric vortex dipoles with rectilinear trajectories aligned with the x -direction of the vertical symmetry plane (Fig. 1). Such controlled laminar experiments are reproducible and allow different measurements to be compared at the same reference times even if not performed simultaneously.

Flow visualizations and Particle Imaging Velocimetry (PIV) measurements have been performed in horizontal and vertical planes with a pulsed laser (30 mJ) and digital camera (12 bit, $1,280 \times 1,024$ pixels). The horizontal plane is set at height $z = 2.2 \text{ cm}$ close to the free surface ($H = 2.5 \text{ cm}$). The vertical plane at $y = 0$ coincides with the vertical plane of symmetry (Fig. 1). The flow is visualized by planar laser induced fluorescence. Fluorescent dye is directly injected in the bulk of the water layer in the vicinity of the flaps and in front, about two minutes before the start of the experiments. Painting the dye directly on the flaps only visualizes the two primary vortices of the dipole. Injecting the dye in the bulk of the fluid and downstream from the flaps, on the other hand, allowed the other flow

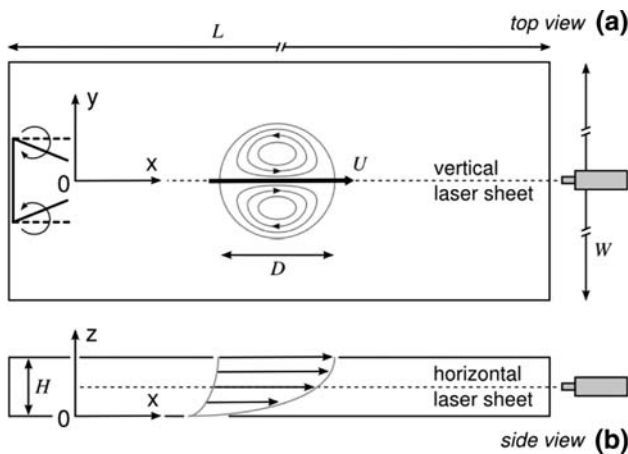


Fig. 1 Experimental setup: top (a) and side (b) views. The sketch is not to scale

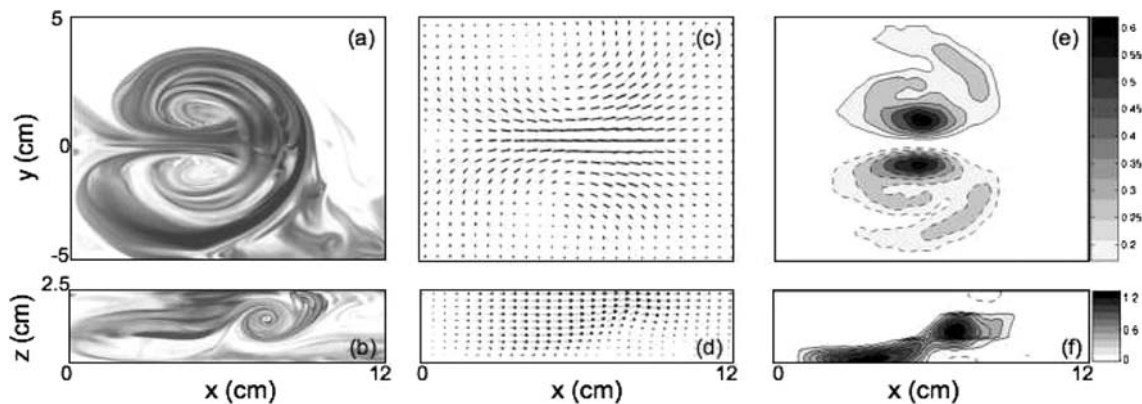


Fig. 2 Horizontal (*top*) and vertical (*bottom*) cross-sections of the flow at $t = 20$ s: dye visualizations (**a**, **b**), PIV-generated velocity field (**c**, **d**) and associated vorticity field (**e**, **f**). The dipole propagates from left to right, at a speed of about 3 mm/s. $H = 2.5$ cm. $T = 10$ s.

The *grayscale color bar* gives the norm of the vorticity in s^{-1} . The positive vorticity is shown by *solid lines*, and negative vorticity by *dashed lines*

structures also to be captured. Figure 2a, b show typical visualizations with such a technique in both the horizontal and vertical planes. For the PIV technique, the flow was seeded with neutrally buoyant, small spherical glass particles whose displacement was analyzed using the correlation image velocimetry technique of Fincham and Spedding (1997). In the following, the initial time $t = 0$ s corresponds to the start of the flaps' rotation, which ends at the closing time $t = T$.

3 Results

Figure 2 shows the structure of the flow at $t = 20$ s for a closing time $T = 10$ s. The main features of the overall flow can be identified from the dye visualizations. The vortex dipole is clearly visible in the horizontal plane (Fig. 2a). This observation is consistent with the horizontal velocity and vertical vorticity fields obtained from the PIV measurements shown in Fig. 2c, e which reveal a pair of counter-rotating horizontal vortices. As suggested by Sous et al. (2004), the dye visualization in the vertical plane of symmetry does indeed reveal the presence of a spanwise vortex located at the front of the dipole (Fig. 2b). Though vortex identification by dye visualization can be misleading for three-dimensional flows, evidence of this spanwise vortex is confirmed by the horizontal vorticity field displayed in Fig. 2f. This demonstrates that such a vortex can be generated in a laminar dipole, in contrast with the experiments of Sous et al. (2004), in which turbulence was suspected to play a role in the formation of the spanwise vortex. The essential features of the dipole and the spanwise vortex have been characterized by Lin et al. (2003). For the case of a sufficiently thin fluid layer, the pattern of vorticity in Fig. 2f is strikingly similar to that shown in

their Figs. 12 and 13. It is noteworthy that the spanwise vortex persists as the dominant structure in the case of deeper fluid layers, for which Lin et al. (2003) observed a hierarchy of horizontally oriented, azimuthal secondary vortices wrapping around the core of the primary vortices.

The flow generated by the self-induced translation of the dipole over the bottom surface produces a boundary layer that can be observed behind the spanwise vortex (Fig. 2f). At this time, the spanwise vortex lies approximately at mid-plane $H/2$ and it is distinct from the boundary-layer vorticity. Moreover, the vorticity field in the horizontal plane in Fig. 2e shows two secondary regions of vertical vorticity around the front of the dipole. This feature can be interpreted as the signature of the spanwise vortex whose side arms seem to be oriented upwards. Such a conjecture has to be confirmed by further experiments. Nevertheless, it suggests that the three-dimensional structure of the spanwise vortex is quite intricate and therefore needs further investigation in order to quantify its influence on the dynamics of the two main vortices that compose the dipole.

The dynamics of the overall structure can be quantified by analyzing the displacement of the dipole as a function of time (Fig. 3). The displacement of the dipole has been measured by following the location of the maximum vorticity in the horizontal plane for two closing times $T = 10$ and 15 s. As in Billant and Chomaz (2000), the curves have been fitted by an exponentially decaying function from which the translation speed of the dipole can be deduced for $t > T$ as follows¹

$$U(t) = U_0 e^{-(t-T)/\tau} \quad (1)$$

¹ Note that such an exponential decay can be theoretically derived (Flór et al. 1995) when considering the diffusion of the classical two-dimensional Lamb–Chaplygin dipole (Meleshko and van Heijst 1994).

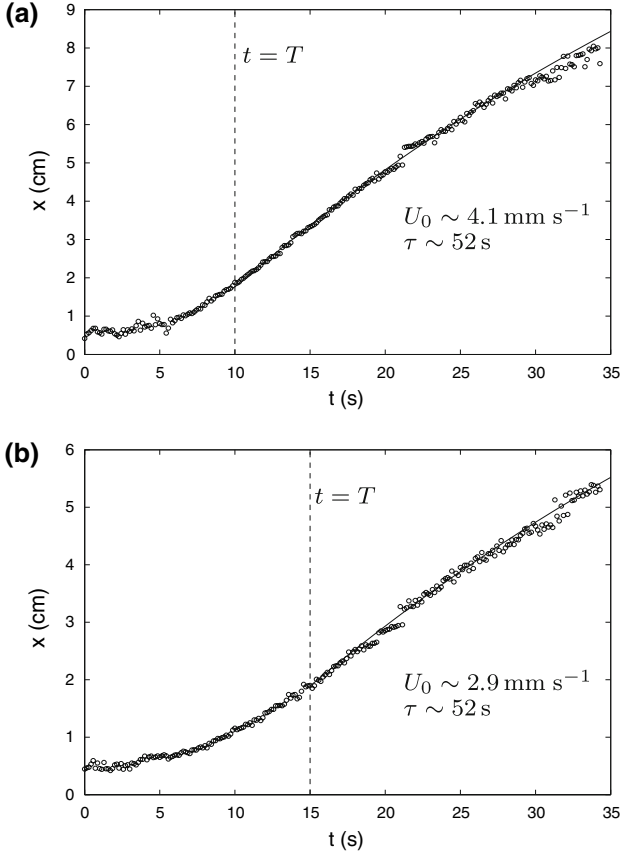


Fig. 3 Displacement of the dipole as a function of time for two closing times (dashed lines) $T = 10$ s (a) and $T = 15$ s (b). The solid line is an exponential fit for $t > T$. $H = 2.5$ cm

where τ corresponds to a decay time of the structure and U_0 denotes the starting velocity of the dipole at the end of the flaps' rotation. These two quantities are computed via a least-square approximation of the experimental data by the exponential law (1). Though the shallow dipole has a non-trivial three-dimensional dynamics, we found that Eq. 1 holds for the present experiments and the exponential fit describes adequately the translation of the dipole as shown in Fig. 3.

As expected, the initial velocity U_0 of the dipole increases as the closing time T is decreased, i.e., when the flaps are closed faster. More precisely U_0 is inversely proportional to the closing time T , in excellent quantitative agreement with Billant and Chomaz (2000) who use the same dipole generating apparatus and predict propagation speeds U_0 of about 4.1 mm/s and 2.7 mm/s for $T = 10$ s and 15 s respectively (extrapolation of their Fig. 4a). Note that these values have been obtained by Billant and Chomaz (2000) for much larger height-to-width aspect ratios, thus suggesting that friction on the no-slip bottom plays a minor role on the dipole starting velocity. The starting velocity seems to be mainly controlled by the flaps

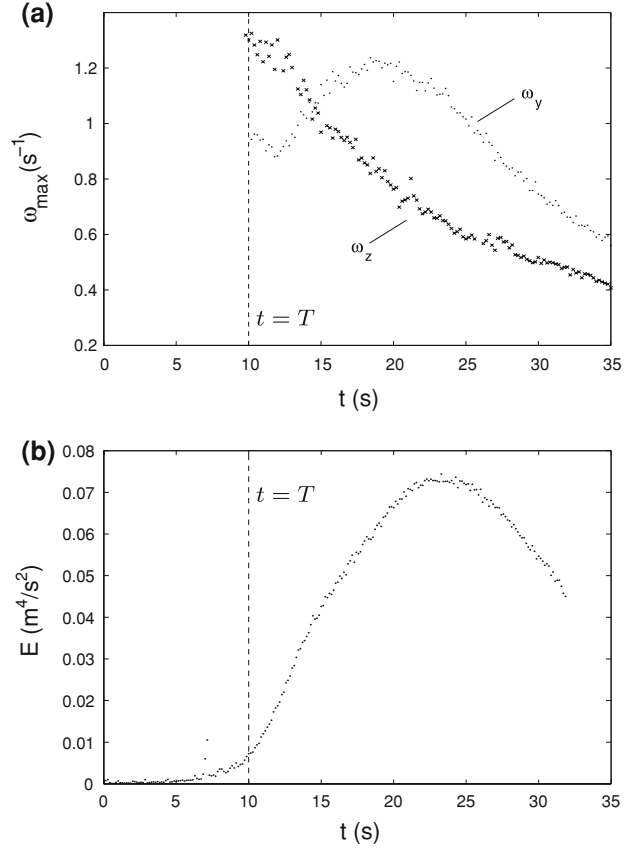


Fig. 4 Time evolution of the maximum vertical (ω_z) and horizontal (ω_y) vorticity (a). Vertical kinetic energy in the vertical plane of symmetry (b). $H = 2.5$ cm, $T = 10$ s

geometry and closing time T , at least for the present set of parameters.

On the other hand, the decay time does not vary with T . The measured value of $\tau \sim 52$ s in both cases ($T = 10$ s and $T = 15$ s) is smaller than previous values obtained for large aspect ratios $\eta > 1$, for which the solid bottom has a negligible influence on the dipole dynamics. For example, Billant and Chomaz (2000) measured a decay time of about 90 s. In the present experiments, the boundary layer is expected to significantly enhance the viscous dissipation of the overall structure, hence we expect a relative reduction of the decay time τ . The influence of the spanwise vortex on the time evolution of the dipole propagation speed is difficult to delimit. Nevertheless, as mentioned by one reviewer, it can be noticed that the turned-up side arms of the spanwise vortex, visible on Fig. 2e, induce a velocity field that tends to bring the dipole vortices closer and also to promote their propagation speed. It is not clear however to what extent this effect quantitatively impedes the resisting influence of friction. An exhaustive parametric study including different depths experiments and 3D PIV measurements is planned in order to address this issue.

A quantitative analysis of the spanwise vortex is proposed in Fig. 4 for $T = 10$ s. Figure 4a compares the temporal evolution of the maxima of the vertical vorticity ω_z and of the horizontal vorticity ω_y . The vertical ω_z vorticity measured in the horizontal plane is a direct measure of the counter-rotating vortices that compose the dipole. This quantity monotonically decreases with time due to viscous diffusion. As suggested by one reviewer, we have checked that the time evolution of the vertical vorticity component closely follows the “universal” decay of vorticity in dipoles discussed by Voropayev et al. (2008). These authors present experiments of dipoles in a decaying stratified turbulence and their measurements confirm that the dipole vorticity decays with time as t^{-1} irrespective of the turbulence intensity, a result that can be deduced from dimensional arguments. It is noteworthy that our present results show a good agreement with this prediction, even though the dipolar flow evolves in a completely different environment. Such a decaying law may arise similarly in both studies because the characteristic vertical lengthscale of the flow is fixed in both cases.

The horizontal vorticity ω_y measured in the vertical plane of symmetry (Fig 4a) does not distinguish between the boundary-layer vorticity at the bottom wall and the vorticity associated with the spanwise vortex. The former dominates just after closing time, while decreasing due to the dissipation of the overall structure. The latter stands out in turn after $t \sim 12$ s as the spanwise vortex grows, reaching a maximum at $t \sim 20$ s before eventually decreasing. It is noteworthy that the vorticity within the spanwise vortex reaches values as high as twice the vertical vorticity associated with the dipole. This suggests that the presence of the spanwise vortex cannot be reduced to a mere perturbation of an otherwise quasi-two-dimensional vortex dipole: it alters the structure and dynamics of the flow at leading order and cannot be neglected. Finally such relative levels of horizontal and vertical vorticity have also been measured for the main azimuthal vortex in the experiments of Lin et al. (2003), an additional evidence that this latter structure is possibly related to the present spanwise vortex.

The horizontal vorticity ω_y in the vertical plane of symmetry mixes both the boundary layer vorticity, with which a quasi-2D approximation of the flow is consistent, and the spanwise vortex, whose formation clearly contradicts the quasi-two-dimensional hypothesis. One way of discriminating between these two sources of horizontal vorticity is to analyze the vertical kinetic energy $E = \int u_z^2 dS$ computed over the whole velocity field in the vertical plane of symmetry (Fig. 4b). This global quantity directly quantifies the vertical motions of fluid, with which the boundary layer is not directly associated. Therefore, it allows the spanwise vortex to be quantitatively identified while providing with a relatively unbiased measure of the

departure from the quasi-two-dimensional approximation classically used for such shallow flows. Confirming the analysis of the previous observations, this quantity increases as the spanwise vortex matures until time $t \sim 23$ s, before decreasing due to the decay of the spanwise vortex and the overall dissipation.

As shown in Fig. 4a, b, the intensity of the spanwise vortex has decreased by at least a factor 2 at time $t \sim 35$ s, with a trend that suggests that its dynamics is mainly controlled at that time by the viscous decay of the global structure. Therefore, the present experiments allowed the main stages of the spanwise vortex development to be covered. By the end of the experiments, this structure is expected to have reached a final decaying, diffusing state.

4 Discussion

The generation process of the spanwise vortex can be dissected qualitatively by invoking basic mechanisms of vorticity dynamics. The first ingredient lies in the specific strain induced by the vortex dipole. It is characterized by a horizontal spanwise stretching field $\partial u_y / \partial y$ with a wide region of large positive values at the front of the dipole (Fig. 5a). In particular, it can be seen that this spanwise stretching is maximal in the vertical plane of symmetry $y = 0$. The second ingredient is directly associated with the no-slip condition at the bottom and the subsequent boundary layer generated by the translation of the dipole. As shown in Fig. 5b, this boundary layer is a source of horizontal spanwise vorticity ω_y that is constantly subjected to the strain field of the vortex dipole. Under such conditions, the magnitude of the spanwise vorticity ω_y is likely to be intensified by the positive stretching $\partial u_y / \partial y > 0$ at the front of the dipole. The dipole intensity and the associated stretching increase as one moves away from the bottom. Therefore, the vorticity is differentially intensified, with larger amplifications for higher fluid layers. Thus, the spanwise vorticity maximum, initially associated to the boundary layer and therefore lying at the bottom, is expected to depart from the wall and move upwards. This vorticity stretching eventually concentrates the boundary-layer vorticity in the form of a distinct spanwise vortex. Such an evolution of the spanwise vorticity ω_y is clearly visible in the time sequence displayed in Fig. 5b, where a spanwise vortex forms from the upper part of the boundary layer. Note that this process is potentially coupled with and promoted by a boundary layer separation at the front of the dipole. Indeed the dipole that translates in a quiet fluid induces an adverse pressure gradient ahead of the boundary layer generated under the propagating structure. Such a configuration is favorable to the separation of

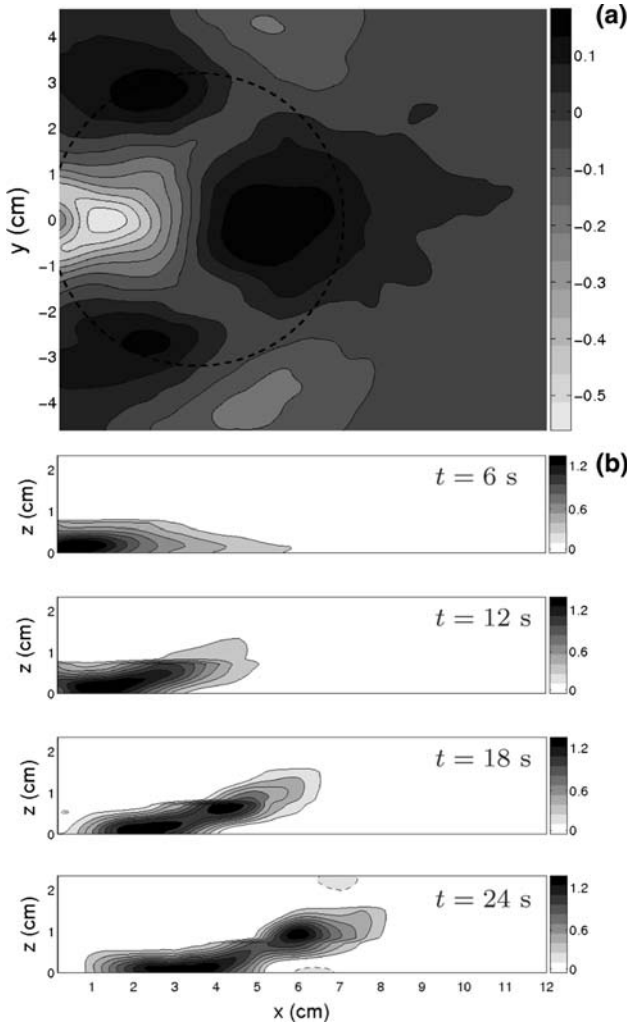


Fig. 5 Contours of the stretching field $\partial u_y / \partial y$ induced by the dipolar structure in a horizontal plane at $t = 12$ s (a). Black and white areas correspond to positive (max. 0.2 s^{-1}) and negative (min. -0.5 s^{-1}) values, respectively. Horizontal vorticity ω_y in the vertical plane of symmetry at the early stages of the spanwise vortex formation (b) (black: 1.4 s^{-1} , white: 0 s^{-1}). $H = 2.5 \text{ cm}$, $T = 10 \text{ s}$

the boundary layer, a phenomenon that could accompany the spanwise vortex formation process by stretching.

Finally, the characteristic radius a of the spanwise vortex can be classically evaluated from a balance between viscous diffusion and strain $\gamma \sim UID$, i.e., $a \sim \sqrt{\nu/\gamma}$. This corresponds to the same scaling as the boundary layer thickness δ , $a \sim H/\sqrt{Re}$ with a typical value of about 5 mm in adequate agreement with the experimental observations (Fig. 2f).

5 Conclusion

Laboratory experiments have been conducted to study the evolution of shallow vortex dipoles. Laminar dipoles were

generated by the controlled rotation of vertical flaps in a thin layer of water. Flow visualizations and Particle Imaging Velocimetry measurements have been performed in horizontal and vertical planes. Both techniques allowed a spanwise vortex structure to be identified and quantitatively characterized. This spanwise vortex lies in front of the dipole, between the two primary vortices, in radical contradiction with the quasi-two-dimensional hypothesis classically used for such shallow flows. The present study focused on the formation and maturation of the spanwise vortex in order to provide with a tentative explanation of its physical origin. The analysis suggests that the spanwise vortex is generated via a differential vortex stretching mechanism triggered by the horizontal strain field of the dipole. The strain field at the front of the dipole stretches the horizontal vorticity associated with the boundary layer generated at the no-slip bottom under the propagating dipole. Such a stretching intensifies the horizontal vorticity and eventually leads to the formation of a distinct spanwise vortex. This phenomenon is potentially accompanied by a boundary-layer separation process due to the adverse pressure gradient induced at the front of the dipole by its propagation in a quiet fluid. We conjecture that such a basic mechanism is not restricted to shallow vortex dipoles, but is potentially active whenever vorticity is available to be stretched by a dipolar structure such as dipoles in Couette flow, or pancake dipoles in a stratified fluid.

Vortex dipoles are recurrent features of natural shallow water flows, such as estuaries or rip currents. Replications of exact oceanic or coastal conditions were not attempted here, as in typical laboratory modeling of geophysical phenomena. We rather focused on the basic processes in the laminar, controlled case. Indeed, as classically put forward, any insight gained into the dynamics of laminar flows can prove useful for improving the comprehension of the behavior of the large-scale coherent structures when considering their turbulent counterpart. Thus, the study of the laminar dynamics can reveal generic mechanisms (such as vortex stretching here) that might also be active on the large-scale structures of the flow even in the presence of turbulence. Moreover, direct quantitative comparisons with the natural, turbulent cases are delicate, even through the use of an eddy viscosity, because the data, such as height-to-width aspect ratios H/D , are not easily available. Nevertheless, these natural dipoles are expected to have aspect ratios less than unity, suggesting that the vertical confinement has a major influence on or even controls the dynamics of the large-scale structures of the flow. In that context, the present experiments are at least qualitatively relevant since they have been designed to include this fundamental characteristic feature.

Future experiments will focus on the influence of the spanwise vortex on the propagation, dissipation rate and

mixing and transport properties of the shallow vortex dipole. The long-time behavior of the flow, and of the spanwise vortex in particular, is also an interesting issue, that ought to be addressed by further studies. Finally, the intricate details of the topology of the overall structure will be investigated in the near future through the development of a three-dimensional PIV technique.

Acknowledgments The authors would like to thank Météo-France for the kind loan of the dipole generating equipment.

References

- Afanasyev YD, Korabel VN (2006) Wakes and vortex streets generated by translating force and force doublet: laboratory experiments. *J Fluid Mech* 553:119
- Akkermans RAD, Kamp LPJ, Clercx HHH, van Heijst GJF (2008a) Intrinsic three-dimensionality in electromagnetically driven shallow flows. *Europhys Lett* 83:24001
- Akkermans RAD, Cieslik AR, Kamp LPJ, Trieling RR, Clercx HJH, van Heijst GJF (2008b) The three-dimensional structure of an electromagnetically generated dipolar vortex in a shallow fluid layer. *Phys Fluids* 20:116601
- Billant P, Chomaz JM (2000) Experimental evidence for a new instability of a vertical columnar vortex pair in a strongly stratified fluid. *J Fluid Mech* 418:167
- Fincham AM, Spedding GR (1997) Low cost, high resolution DPIV for measurement of turbulent fluid flow. *Exp Fluids* 23:449
- Flór JB, van Heijst GJF, Delfos R (1995) Decay of dipolar vortex structures in a stratified fluid. *Phys Fluids* 7:374
- Fujiwara T, Nakata H, Nakatsuji K (1994) Tidal-jet and vortex-pair driving of the residual circulation in a tidal estuary. *Continental Shelf Res* 14:1025
- Leweke T, Williamson CHK (1998) Cooperative elliptic instability of a vortex pair. *J Fluid Mech* 360:85
- Lin JC, Ozgoren M, Rockwell D (2003) Space-time development of the onset of a shallow-water vortex. *J Fluid Mech* 485:33
- Meleshko VV, van Heijst GJF (1994) On Chaplygin's investigations of two-dimensional vortex structures in an inviscid fluid. *J Fluid Mech* 272:157
- Meunier P, Leweke T (2005) Elliptic instability of a co-rotating vortex pair. *J Fluid Mech* 533:125
- Peregrine DH (1998) Surf zone currents. *Theor Comput Fluid Dyn* 10:295
- Smith JA, Largier JL (1995) Observations of nearshore circulations: rip currents. *J Geophys Res* 100:10967
- Sous D, Bonneton N, Sommeria J (2004) Turbulent vortex dipoles in a shallow water layer. *Phys Fluids* 16:2886
- Voropayev SI, Afanasyev YaD, Filipov IA (1991) Horizontal jets and vortex dipoles in a stratified fluid. *J Fluid Mech* 227:543
- Voropayev SI, Fernando HJS, Smirnov SA, Morrison R (2007) On surface signatures generated by submerged momentum sources. *Phys Fluids* 19:076603
- Voropayev SI, Fernando HJS, Morrison R (2008) Dipolar eddies in a decaying stratified turbulent flow. *Phys Fluids* 20:026602
- Wells MG, van Heijst GJF (2003) A model of tidal flushing of an estuary by dipole formation. *Dyn Atmos Oceans* 37:223